Bioorganic & Medicinal Chemistry Letters 21 (2011) 3726–3729

Contents lists available at ScienceDirect

Bioorganic & Medicinal Chemistry Letters

journal homepage: www.elsevier.com/locate/bmcl

Highly selective c-Jun N-terminal kinase (JNK) 3 inhibitors with in vitro CNS-like pharmacokinetic properties II. Central core replacement

R. Jeffrey Neitz [a,*], Andrei W. Konradi [a], Hing L. Sham [a,b], Wes Zmolek [d], Karina Wong [d], Ann Qin [d], Colin Lorentzen [d], David Nakamura [d], Kevin P. Quinn [d], John-Michael Sauer [d], Kyle Powell [e], Lany Ruslim [e], David Chereau [e], Zhao Ren [e], John Anderson [e], Frédérique Bard [e], Ted A. Yednock [a,b,c,d,e], Irene Griswold-Prenner [e]

[a] Department of Medicinal Chemistry, Elan Pharmaceuticals, 180 Oyster Point Boulevard, South San Francisco, CA 94080, United States
[b] Department of Process and Analytical Chemistry, Elan Pharmaceuticals, 180 Oyster Point Boulevard, South San Francisco, CA 94080, United States
[c] Department of Molecular Design, Elan Pharmaceuticals, 180 Oyster Point Boulevard, South San Francisco, CA 94080, United States
[d] Department of Lead Finding, Drug Disposition, and Safety Evaluation, Elan Pharmaceuticals, 800 Gateway Boulevard, South San Francisco, CA 94080, United States
[e] Department of Biology, Elan Pharmaceuticals, 1000 Gateway Boulevard, South San Francisco, CA 94080, United States

ARTICLE INFO

Article history:
Received 12 January 2011
Revised 15 April 2011
Accepted 19 April 2011
Available online 27 April 2011

ABSTRACT

In this Letter, we describe the evolution of selective JNK3 inhibitors from **1**, that routinely exhibit >10-fold selectivity over JNK1 and >1000-fold selectivity over related MAPKs. Strong SAR was found for substitution of the naphthalene ring, as well as for inhibitors adopting different central scaffolds. Significant potency gains were appreciated by inverting the polarity of the thione of the parent triazolothione **1**, resulting in potent compounds with attractive pharmacokinetic profiles.

The c-Jun N-terminal kinases (JNKs 1–3) are serine/threonine targeted members of the mitogen-activated protein kinases (MAPKs).[1] JNK3 is concentrated primarily in the brain while JNK1 and JNK2 are distributed widely. JNK1 performs important functions in maintenance and regulation of the central nervous system (CNS), and has been of interest as a target for inhibition in the periphery to impact metabolic disorders.[2] JNK2, JNK3, and dual JNK2 and JNK3 knockout mice all show phenotypic resistance to induced neurodegeneration.[3] Inhibition of JNK2 and JNK3 thus may provide a means to directly impact Alzheimer's disease and Parkinson's disease, among others.[4]

Compound **1** was identified from our in-house compound collection during a screening campaign to identify compounds with JNK activity, and broad selectivity against other kinases (Fig. 1). SAR for the triazolone variants of **1** have been previously disclosed.[5] Herein we describe variously substituted naphthyls and pyridyls appended to the triazolothione, as well as the substitution of the central ring by a series of heterocycles.

Exploration of the SAR began by substituting the napthyl ring with quinolines in an attempt to ameliorate glucuronidation and enhance potency, while retaining the excellent solubility and p450 stability. Syntheses of these analogs were accomplished using the two-step procedure described in Scheme 1. Each quinoline derivative lost nearly all activity versus the JNKs (Table 1). Substitution off the pyridyl ring was also explored. Again the SAR here was very sharp, with a 30× loss in JNK3 activity seen with the addition of a simple methyl group to the γ-position (**5**).

JNK3 IC_{50} = 1.07uM
JNK2 IC_{50} = 7.28uM
JNK1 IC_{50} = 2.95uM
OxMet (%R): m=100, h=100
GlucMet (%R) = m=1, h=8
P-gp Efflux = 1.12
solubility = 100uM

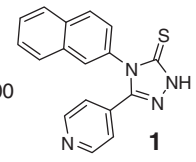

1

Figure 1. JNK3 kinase inhibitor: screening hit.[6,7]

Potency gains were appreciated here for derivatives with nitrogen substitution at the γ-position (as was similarly the case with the triazolone derivatives disclosed previously),[5] albeit at the expense of solubility.

Having determined useful appendages for increasing target potency, we next set about to probe the triazolothione core (Table 2). To our surprise, replacing the triazolothione with a simple triazole (**14**) resulted in only a 10× loss in potency. Indeed, this triazole was 3× more potent than the parent triazolone.[5]

Synthesis of the most active analog **14** was accomplished in two steps (Scheme 2).

Next, wholesale substitution of the central ring with other heterocycles was explored (Table 3).

Various regiochemical permutations of pyrazoles, triazoles, and a tetrazole were synthesized and found to exhibit a

* Corresponding author.
E-mail address: jeff.neitz@gmail.com (R. Jeffrey Neitz).

0960-894X/$ - see front matter © 2011 Elsevier Ltd. All rights reserved.
doi:10.1016/j.bmcl.2011.04.074

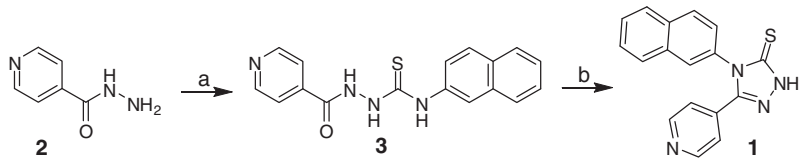

Scheme 1. Reagents and conditions: (a) 2-naphthylisothiocyanate, MeOH, 70 °C, microwave, 15 min; (b) 5% KOH aq, 110 °C, microwave, 15 min (75% overall).

Table 1
SAR of triazolothiones[a]

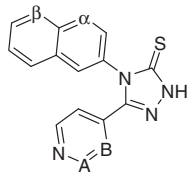

#	α	β	A	B	JNK3 IC_{50}	JNK2 IC_{50}	JNK1 IC_{50}	Soln
1	C–H	C–H	C–H	C–H	0.559	2.98	12.5	100
4	N	C–H	C–H	C–H	>50	>50	>50	100
5	C–H	C–H	C–Me	C–H	14.8	15.3	>50	100
6	N	C–H	C–Me	C–H	>50	>50	>50	100
7	C–H	C–H	C–H	C–F	27.4	34.6	>50	35
8	C–H	C–H	C–Br	C–H	>50	>50	>50	35
9	C–H	N	C–H	C–H	31.8	>50	>50	15
10	C–H	C–H	C–NH_2	C–H	1.03	0.504	24.3	100
11	C–H	C–H	CNH-cHex	C–H	0.0522	0.0665	>50	5
12	C–H	C–H	C–NH-methylcProp	C–H	0.945	2.25	>50	35

[a] Values are in μM and means of at least three experiments at 10 μM ATP concentration.

Table 2
SAR of triazole perturbations[a]

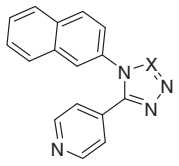

#	X	JNK3 IC_{50} (μM)	JNK2 IC_{50} (μM)	JNK1 IC_{50} (μM)	Solubility (μM)
1	C–SH	0.559	2.98	12.5	100
13	C–CF_3	>50	>50	>50	15
14	C–H	4.48	19.0	>50	35
15	C–Me	18.3	46.2	>50	100
16	N	49.1	>50	>50	15
17	C–Cl	30.4	>50	>50	78
18	C–N–NH_2	14.9	34.0	>50	65

[a] Values are means of at least three experiments at 10 μM ATP concentration.

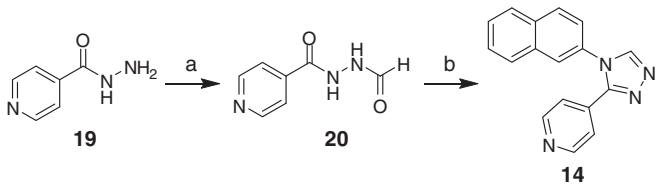

Scheme 2. Reagents and conditions: (a) ethylformate (10 equiv), 110 °C (45%); (b) 2-aminonaphthalene, MeOH, 110 °C (63%).

relatively flat SAR, excepting the potency gains seen for the H-bond donating triazole **28** and pyrazole **29**. These analogs also retained 20× selectivity over JNK1, however oxidative metabolism was pervasive.

Attempts to substitute the five-membered ring core with a six-membered pyrimidine scaffold failed to track in potency (Table 4). Both **29** and **31** were accessed from intermediate **36** (Scheme 3).

Permeability and P-gp efflux are both critical in vitro measures to evaluate the potential of a molecule to access the parenchyma of the brain and be an effective CNS therapeutic. Table 5 illustrates the moderation of these properties for our most potent compounds. Moderate metabolic stability was observed in a microsomal assay. Metabolism via glucuronidation was not found to be a problem.

In summary, we have succeeded in replacing the triazolothione core of the screening hit with simple pyrazole which shows moderate CNS properties with a 2× increase in potency.

Table 3
SAR of scaffold variation[a]

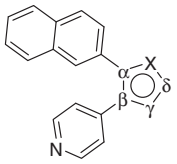

#	α	β	γ	δ	X	JNK3 IC_{50} (μM)	JNK2 IC_{50} (μM)	JNK1 IC_{50} (μM)	Ox. Met[b] (%m, %h)
21	C	N	N–H	N	C–Cl	12.6	37.9	>50	0, 5
22	C	N	N–H	N	C–H	4.81	18.6	>50	0, 12
23	C	N	N–H	C–H	C–H	2.46	9.31	41.9	0, 2
24	N	C	C–H	C–H	N	1.23	4.88	>50	11, 58
25	C	N	N–H	N	N	>50	>50	>50	0, 16
26	N	C	N–H	C–H	C–H	1.91	6.39	>50	0, 18
27	N	C	C–H	N	N	2.67	9.14	>50	n/a
28	C	C	N–H	N	N	0.364	1.22	6.85	2, 44
29	C	C	C–H	N–H	N	0.245	0.864	7.15	1, 52

[a] Values are means of at least three experiments at 10 μM ATP concentration.
[b] Percent remaining after 30 min incubation with liver microsomes (m = mouse and h = human).

Table 4
SAR of pyrimidyl scaffold[a]

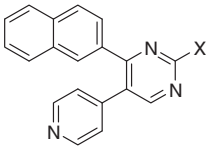

#	X	JNK3 IC_{50}	JNK2 IC_{50}	JNK1 IC_{50}	OxMet[b] (m, h)
31	H	4.13	18.1	>50	0, 29
32	OH	1.51	3.89	31.8	72, 76

[a] Values are in μM and means of at least three experiments at 10 μM ATP concentration.
[b] Percent remaining after 30 min incubation with liver microsomes (m = mouse and h = human).

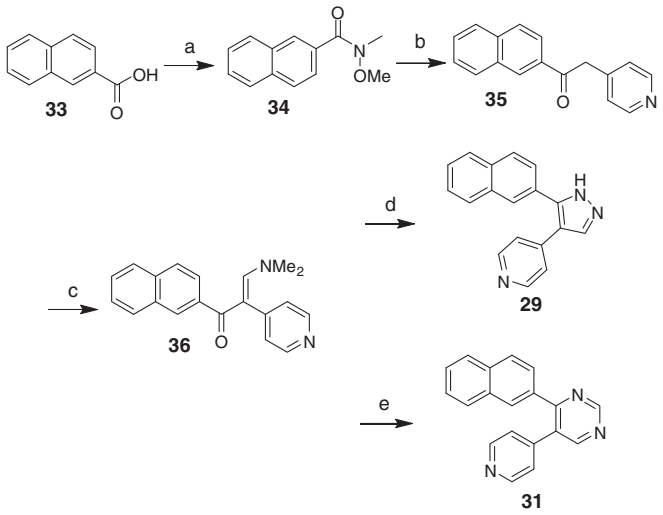

Scheme 3. Reagents and conditions: (a) (1) oxaloylchloride, (2) HN(OMe)Me (80%); (b) LDA, 4-methylpyridine, 0 °C (65%); (c) DMF/DMA (2 equiv), DCE; (d) hydrazine, 90 °C (70% for two steps); (e) amidine 90 °C (35% for two steps).

Acknowledgments

We would like to thank Michael P. Bova, Danny Tam, Sarah Wright, Carla Ramos, and Robert Arslanian for their contributions to this work.

Table 5
In vitro pharmacokinetic properties

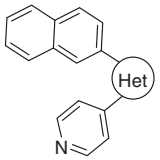

#	Het	JNK3 IC_{50} μM	P_{app}[6] (nm/s)	OxMet GlucMet (m, h)[a]	P-gp[6] efflux
29		0.245	169	1, 52 100, 73	1.14
28		0.364	152	45, 44 n/a	n/a
14		4.48	306	76, 100 87, 100	n/a
22		4.81	379	22, 12 90, 78	n/a
32	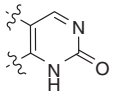	1.51	165	80, 76 n/a	n/a

[a] Percent remaining after 30 min incubation with liver microsomes for ox. and 60 min for gluc. (m = mouse and h = human).

Supplementary data

Supplementary data associated with this article can be found, in the online version, at doi:10.1016/j.bmcl.2011.04.074.

References and notes

1. (a) Siddiqui, M. S.; Reddy, P. A. *J. Med. Chem.* **2010**, *53*, 3005; (b) Bogoyevitch, M. A.; Ngoei, K. R. W.; Zhao, T. T.; Yeap, Y. Y. C.; Ng, D. C. H. *Biochim. Biophys. Acta* **2010**, *1804*, 463; (c) Haeusgen, W.; Boehm, R.; Zhao, Y.; Herdegen, T.; Waetzig, V. *Neuroscience* **2009**, *161*, 951; (d) LoGrasso, P.; Kamenecka, T. *Mini-Rev. Med. Chem.* **2008**, *8*, 755; (e) Bogoyevitch, M. A.; Arthur, P. G. *Biochim. Biophys. Acta* **2008**, *1784*, 76; (f) Bogoyevitch, M. A.; Kobe, B. *Microbiol. Mol. Biol. Rev.* **2006**, *70*, 1061; (g) Karin, M.; Gallagher, E. *IUBMB Life* **2005**, *57*, 283.
2. Chang, L.; Jones, Y.; Ellisman, M. H.; Goldstein, L. S.; Karin, M. *Dev. Cell* **2003**, *4*, 521.

3. (a) Hunot, S.; Vila, M.; Teismann, P.; Davis, R. J.; Hirsch, E. C.; Przedborski, S.; Rakic, P.; Flavell, R. A. *Proc. Natl. Acad. Sci. U.S.A.* **2004**, *101*, 665; (b) Yang, D. D.; Kuan, C.-Y.; Whitmarsh, A. J.; Rincón, M.; Zheng, T. S.; Davis, R. J.; Rakic, P.; Flavell, R. A. *Nature* **1997**, *389*, 865.
4. (a) Borsello, T.; Forloni, G. *Curr. Pharm. Des.* **2007**, *13*, 1875; (b) Wang, W.; Ma, C.; Mao, Z.; Li, M. *Drug News Perspect.* **2004**, *17*, 646; (c) Resnick, L.; Fennell, M. *Drug Discovery Today* **2004**, *9*, 932; (d) Harper, S. J.; Wilkie, N. *Expert Opin. Ther. Targets* **2003**, *7*, 187; (e) Manning, A. M.; Davis, R. J. *Nat. Rev. Drug Discov.* **2003**, *2*, 554.
5. Probst, G. P.; Bowers, S.; Sealy, J. M.; Truong, A. P.; Hom, R. K.; Galemmo, Robert A.; Konradi, A. K.; Sham, H. L.; Quincy, D. A.; Pan, H.; Yao, N.; Lin, M.; Toth, G.; Artis, D. R.; Zmolek, W.; Wong, K.; Qin, A.; Lorentzen, C.; Nakamura, D. F.; Quinn, K. P.; Sauer, J.-M.; Powell, K.; Ruslim, L.; Wright, S.; Chereau, D.; Ren, Z.; Anderson, J. A.; Bard, F.; Yednock, T. A.; Griwold-Prenner, I. *Bioorg. Med. Chem. Lett.* **2011**, *21*, 315.
6. For conditions of in vitro pharmacokinetic assays, see: Truong, A. P.; Aubele, D. A.; Probst, G. D.; Neitzel, M. L.; Semko, C. M.; Bowers, S.; Dressen, D.; Hom, R. K.; Konradi, A. W.; Sham, H. L.; Garofalo, A. W.; Keim, P. S.; Wu, J.; Dappen, M. S.; Wong, K.; Goldbach, E.; Quinn, K. P.; Sauer, J.-M.; Brigham, E. F.; Wallace, W.; Nguyen, L.; Hemphill, S. S.; Bova, M. P.; Basi, G. *Bioorg. Med. Chem. Lett.* **2009**, *19*, 4920.
7. Details of the TR-FRET enzyme inhibition assay may be found in the Supplementary data for Hom, R. K. et al *Bioorg. Med. Chem. Lett.* **2009**, *20*, 7303. Kinase selectivity data for **1** can be found in the Supplementary data.